Quantum search with interacting Bose-Einstein condensates

Mahdi Ebrahimi Kahou and David L. Feder*
Institute for Quantum Information Science and Department of Physics and Astronomy, University of Calgary, Calgary T2N 1N4, Alberta, Canada
(Received 15 March 2013; published 11 September 2013)

One approach to the development of quantum search algorithms is the quantum walk. A spatial search can be effected by the continuous-time evolution of a single quantum particle on a graph containing a marked site. In many physical implementations, however, one might expect to have multiple particles. In interacting bosonic systems at zero temperature, the dynamics is well described by a discrete nonlinear Schrödinger equation. We investigate the role of nonlinearity in determining the efficiency of the spatial search algorithm within the quantum walk model, for the complete graph. The analytical calculations reveal that the nonlinear search time scales with the size of the search space N like $\sqrt{N}$, equivalent to the linear case, though with a different overall constant. The results indicate that interacting Bose-Einstein condensates at zero temperature could be natural systems for implementation of the quantum search algorithm.

DOI: 10.1103/PhysRevA.88.032310 PACS number(s): 03.67.Ac, 03.75.Kk, 03.65.Xp

I. INTRODUCTION

Searching is arguably one of the most important problems in computer science. The search problem consists of finding a particular (marked) element in a set containing N items. The simplest classical approach is to uniformly sample the set until the marked element is found, which on average occurs in a time $t = O(N)$. Though the sampling can be recast into the framework of Markov chains, the $O(N)$ scaling of the classical search time is optimal.

Grover [1,2] constructed an algorithm based on quantum mechanics that can find the marked element of a set quadratically faster, in a time $t = O(\sqrt{N})$. This was proven to be optimal [3]. The quantum search algorithm can be recast in terms of quantum walks, the quantum mechanical extension to Markov chains. The origins of the discrete-time quantum walk can be traced to Meyer [4,5], and the concept was further developed in 2001 by several others [6–8]. The continuous-time quantum walk, the quantum analog of a continuous-time Markov process, was introduced by Farhi and Gutmann [9] and extended by them and Childs [10]. Numerous algorithms based on quantum walks were soon developed that were shown to be more efficient than the best-known classical algorithms [11–15]. Among these are quantum walk search algorithms, based both on the discrete-time quantum walk [16–20] and on the continuous-time quantum walk [21–23]. In these approaches, the set corresponds to the vertices of a graph, and the marked element is one distinguishable vertex. While the spatial search time attains the optimal scaling in most graphs, including the complete graph, complete bipartite graphs, m-partite graphs [20], the hypercube [16], the Johnson graph [24], and regular lattices with dimension $\geqslant 3$ [22], it remains at best $t = O(\sqrt{N \log N})$ for quantum walks in the two-dimensional square lattice despite much effort [18,22,25,26], and $t = O(N)$ in one dimension.

Quantum walks have been realized using a variety of experimental approaches. Some of the earliest experiments were based on nuclear magnetic resonance [27,28]. Three steps in a discrete-time quantum walk were realized with $^{25}Mg^{+}$ ions in a linear Paul trap [29]; longer quantum walks were effected more recently with $^{40}Ca^{+}$ ions [30]. Five steps in a quantum walk were implemented using passive optical elements [31,32]. Quantum walks have also been implemented with single neutral ^{133}Cs atoms [33] confined in optical lattices [34].

Because the behavior of quantum walks is governed by quantum interference, it is not necessary to restrict physical systems to single walkers. For example, a quantum walk with two identical photons was demonstrated using evanescently coupled wave guides [35,36]. In fact, there are several indications that quantum walks with multiple indistinguishable particles have unique properties. Nonclassical correlations arise between two noninteracting photonic walkers [36–40]. Two-photon quantum walks with conditioned interactions and strong nonlinearities were recently reported [41]. Quantum walks have also been realized using Bose-Einstein condensates (BECs) of ^{87}Rb [42]. Some classically intractable problems, such as boson sampling, are efficiently solved using quantum walks with multiple indistinguishable bosons [43,44]. Theoretical work suggests that multiple indistinguishable walkers could help determine if two graphs are isomorphic, with interactions improving the power of the algorithm [45–47]. For suitably defined graphs, quantum walks with multiple interacting walkers are able to perform arbitrary quantum algorithms [48].

Large numbers of indistinguishable bosons at low temperatures can form a BEC. Implementing a continuous-time quantum walk using BECs is equivalent to allowing the bosons to evolve under a governing lattice or graph Hamiltonian. In the presence of weak particle interactions, the resulting Gross-Pitaevskii (GP) equation of motion in the mean-field approximation is nonlinear [49]. In principle, the presence of nonlinearity in quantum dynamics can radically alter the performance of quantum algorithms [50], even allowing NP-complete problems to be solved in polynomial time (NP stands for non-deterministic polynomial time). One might therefore conjecture that the time scale for the quantum search problem could be modified by the presence of nonlinearity. That said, the nonlinearity that appears in the GP equation has its origins

*dfeder@ucalgary.ca

in ordinary linear quantum mechanics, which would appear to rule out any improvement in the scaling of the quantum search time with N (though it could always be worse). In any case, it is important to know how the presence of nonlinearity in the governing equations would affect the performance of a quantum search. The influence of (a physically motivated) nonlinearity on the time to effect a quantum walk spatial search is the central question addressed in this work. The results indicate that interacting BECs can indeed implement a quantum spatial search algorithm.

We consider the quantum search algorithm in the complete graph using a continuous-time quantum walk based on the discrete GP equation. In the complete graph, each site or vertex is connected to every other; a boson at a given site can tunnel or hop to any other site with equal probability. While a physical lattice with the connectivity of the complete graph has not yet been realized experimentally, a recent theoretical proposal to simulate the hypercube graph with ultracold atoms [51] suggests that other graphs with unusual connectivity properties might be experimentally feasible in the future. In any case, study of the complete graph offers several theoretical advantages. The search time obtained in the linear quantum walk algorithm has previously been shown to be optimal [21]. The neighborhood of every vertex corresponds to all other vertices, so that the quantum walk naturally mimics a uniform sampling of the set elements. Finally, the symmetry of the complete graph allows the vertex set to be decomposed into two inequivalent elements: the marked vertex and the set of unmarked vertices. This allows the N-dimensional Hilbert space to be reduced to two dimensions, greatly simplifying the analysis of the nonlinear problem.

This paper is organized as follows. In Sec. II we review the continuous-time quantum walk approach to the spatial search problem and derive the associated nonlinear equation of motion for a quantum search based on interacting BECs. The analytical results are presented in Sec. III, and the criteria for a complete search (unit output probability on the marked vertex in the limit of large N) and an incomplete search are derived. The performance of the algorithm in the presence of errors is analyzed numerically in this section. The results are summarized in Sec. IV.

II. BACKGROUND

A. Continuous-time quantum walk search algorithm

In the continuous-time quantum walk, the state of the quantum walker $|\psi\rangle$ is evolved in time by the action of the Hamiltonian $H_0 = -\gamma L$, where L is the Laplacian operator and γ is the transition amplitude. Given an N-dimensional graph $G = (V,E)$, where $V = \{1,2,\ldots,N\}$ and E correspond to the set of vertices and edges, respectively, one can define the Laplacian as $L = A - D$, where $A = A(G)$ is the adjacency matrix associated with graph G and D is a diagonal matrix whose elements are $D_{ii} = \sum_j A_{ij} = \deg(i)$, the degree of vertex i (inclusion of the diagonal is not needed if the graph is regular). The adjacency matrix specifies the graph connectivity and its matrix elements are defined as

$$A_{ij} = \begin{cases} 1 & \text{if} \quad (i,j) \in E, \\ 0 & \text{otherwise.} \end{cases} \tag{1}$$

In the continuous-time quantum walk, one associates each vertex i with a basis vector $|i\rangle$; the set of basis vectors spans the N-dimesional Hilbert space. The state of the quantum walker is $|\psi(t)\rangle = \sum_i a_i(t)|i\rangle$, where $a_i(t)$ are time-dependent complex coefficients. The quantum walk is then effected by performing the unitary transformation $|\psi(t)\rangle = e^{-iH_0 t}|\psi(0)\rangle$ on the particle state vector ($\hbar$ is set to unity in this work).

In the continuous-time quantum walk search algorithm of Childs and Goldstone [21], one of the basis vectors $|w\rangle$ is treated differently. This is accomplished by introducing a marking or oracle Hamiltonian:

$$H_w \equiv -|w\rangle\langle w|. \tag{2}$$

The quantum state is then evolved according to the total Hamiltonian $H = H_0 + H_w$, i.e., $|\psi(t)\rangle = e^{-iHt}|\psi(0)\rangle$. It was shown that if the initial state is chosen to be the uniform superposition of all sites

$$|\psi(0)\rangle = |S\rangle \equiv \frac{1}{\sqrt{N}} \sum_{i=1}^{N} |i\rangle, \tag{3}$$

then there exists a time t_s and value of γ for which the probability at the marked site $|\langle w|\psi(t_s)\rangle|^2 = |\psi_w(t_s)|^2$ will attain unity. For the complete graph, $t_s = \frac{\pi}{2}\sqrt{N}$ and $\gamma = \frac{1}{N}$. For the hypercube and an m-dimensional square lattice for $m > 4$, the search time remains $t_s = O(\sqrt{N})$.

B. Discrete Gross-Pitaevskii equation

A convenient starting point for the description of interacting BECs is the GP equation [49]

$$i\frac{\partial}{\partial t}\Psi(\mathbf{r},t) = \left[-\frac{1}{2m}\nabla^2 + V(\mathbf{r}) + U|\Psi(\mathbf{r})|^2\right]\Psi(\mathbf{r},t), \tag{4}$$

where $V(\mathbf{r})$ is some time-independent external potential, U is the particle interaction strength, and $\Psi(\mathbf{r},t)$ is the BEC wave function. All of the M bosons are assumed to be in the same single-particle state, so the normalization condition is $\int d\mathbf{r}|\Psi(\mathbf{r},t)|^2 = M$. It is convenient to define the BEC wave function in terms of a new wave function, $\Psi(\mathbf{r},t) = \sqrt{M}\psi(\mathbf{r},t)$, so that $\int d\mathbf{r}|\psi(\mathbf{r},t)|^2 = 1$.

Consider functions $V(\mathbf{r})$ corresponding to a series of N potential energy wells, each centered at $\mathbf{r}_j$ with $j = 1,\ldots,N$. A simple example in one dimension would be $V(x) = V_0\cos^2(\pi x/a)$ in a box of length L, where a is some arbitrary length scale and $0 \leqslant x \leqslant L$; if L/a is an integer, the potential minima are found at $x/a = (2n+1)/2$ with n positive integers and $n_{\max} = N = L/a$. If the confinement is sufficiently strong, the particles comprising the BEC will be completely confined to the sites of the potential $V(\mathbf{r})$; reducing the confinement would allow tunneling between nearby sites. The BEC wave function can then be expanded in a basis of Wannier functions $w(\mathbf{r}-\mathbf{r}_j)$ localized to the sites, $\psi(\mathbf{r}) = \sum_j \psi_j w(\mathbf{r}-\mathbf{r}_j)$. Inserting this into Eq. (4), multiplying on the left by $w^*(\mathbf{r}-\mathbf{r}_k)$, and integrating over all space give

$$i\frac{\partial}{\partial t}\psi_k = -\sum_j \gamma_{kj}\psi_j + g_k|\psi_k|^2\psi_k, \tag{5}$$

where

$$\gamma_{kj} = -\int d\mathbf{r} w^*(\mathbf{r}-\mathbf{r}_k)\left[-\frac{1}{2m}\nabla^2 + V(\mathbf{r})\right] w(\mathbf{r}-\mathbf{r}_j) \quad (6)$$

is the amplitude to tunnel between sites centered at $\mathbf{r}_j$ and $\mathbf{r}_k$, and

$$g_k = MU\int d\mathbf{r}|w(\mathbf{r}-\mathbf{r}_k)|^4 \quad (7)$$

is the on-site interaction strength. In deriving Eq. (5), the Wannier functions are assumed to be orthonormal and to be so strongly localized that the spatial integrals of four Wannier functions are insignificant unless all their arguments are the same.

For all the analytical calculations in this work, we make the further simplifying assumption that $\gamma_{kj} = \gamma > 0$ for all nearest neighbors $(j,k) \in E$ and that the particle interactions are site independent, $g_k = g$. For mean-field theory to remain valid, one requires $g/\gamma \lesssim 5.8z$, where z is the site coordination number (vertex degree) in the limit $z \to \infty$ [52,53]. For the complete graph K_N with $N = |V|$ vertices investigated in the present work, each vertex has $z = N-1$ neighbors. Mean-field theory therefore requires $g/\gamma \lesssim N$, which is easy to satisfy for large N.

The discrete GP equation can then be written

$$i\frac{\partial}{\partial t}\psi_k = -\gamma A_{kj}\psi_j + g|\psi_k|^2\psi_k, \quad (8)$$

where A_{kj} are the matrix elements of the graph adjacency matrix A defining the connectivity of the sites. For graphs with constant degree (i.e., site valency) z, the Laplacian is $L = A - D = A - zI$. Because a constant energy offset cannot change the dynamics, the BEC wave function is equivalently described by the GP Hamiltonian

$$H_{\rm GP} = -\gamma L + g\sum_{k=1}^{N}|\psi_k|^2|k\rangle\langle k|, \quad (9)$$

which generates time evolution via the usual Schrödinger equation $i\partial\psi_k/\partial t = \langle k|H_{\rm GP}|\psi\rangle$, where $\psi_k = \langle k|\psi\rangle$. The nonlinear quantum walk search Hamiltonian then takes the following form:

$$H = H_{\rm GP} - |w\rangle\langle w| = -\gamma L - |w\rangle\langle w| + g\sum_{i=1}^{N}|\psi_i|^2|i\rangle\langle i|. \quad (10)$$

For example, in ultracold atom experiments an individual site of an optical lattice could in principle be 'marked' by modifying the local potential using single-site addressing [54].

The simplest (though not the only) way to guarantee that $\gamma_{jk} = \gamma$ is to assume that $|\mathbf{r}_j - \mathbf{r}_k| =$ constant for all nearest neighbors $(j,k) \in E$. The dimension $\dim(G)$ of a graph G is defined as the smallest number d for which the graph satisfying this property can be embedded in d-dimensional Euclidean space $\mathbb{R}^d$. For the special case $d = 2$ these graphs are called unit-distance graphs; examples include cycles, regular two-dimensional lattices, and hypercubes. Of course, the three-dimensional regular lattice also has dimension $d = 3$. The complete graph K_N with $N = |V|$ vertices investigated in the present work unfortunately has dimension $d = N-1$ [55]; the vertices form a d simplex arranged over the d-dimensional hyperspherical surface of circumradius r with fixed distance $r\sqrt{2(N+1)/N}$ [56]. This makes the direct physical realization of the complete graph connectivity via a potential energy function $V(\mathbf{r})$ challenging unless a three-dimensional embedding can be found. In principle, this might be possible by varying the positions of the physical sites while simultaneously changing the potential barrier heights. A much simpler approach would likely be to pursue a photonic implementation employing passive optical elements such as multiple beam splitters [57]. The complete graph is nevertheless interesting from a purely theoretical perspective.

III. NONLINEAR QUANTUM WALK SEARCH IN THE COMPLETE GRAPH

A. Reduction to two dimensions

Consider the action of Hamiltonian (10) for the N-vertex complete graph K_N. The complete graph is associated with the adjacency matrix with elements $A_{ij} = 1 - \delta_{ij}$. The vertex degree is constant $z = N-1$ so the Laplacian is $L = A - (N-1)I = J - NI$, where J is the N-dimensional all-1 matrix. In terms of the initial state $|S\rangle$ defined in Eq. (3), the Laplacian is $L = N|S\rangle\langle S| - NI$. Since $-NI$ corresponds to a constant energy shift it cannot change the dynamics of the system. The Hamiltonian for the quantum walk search, (10), then becomes

$$H = -\gamma N|S\rangle\langle S| - |w\rangle\langle w| + g\sum_{i=1}^{N}|\psi_i|^2|i\rangle\langle i|. \quad (11)$$

In the absence of the nonlinear term, this Hamiltonian corresponds to a two-level operator for states $|S\rangle$ and $|w\rangle$. The Hamiltonian then rotates $|S\rangle$ into $|w\rangle$ in time $t_s \sim \sqrt{N}$ inversely proportional to the two states' overlap $\langle S|w\rangle = 1/\sqrt{N}$.

It would be desirable to express the nonlinear Hamiltonian, (11), as a two-level operator. For the complete graph, the initial condition, (3), can be written as

$$|\psi(0)\rangle = |S\rangle = \frac{1}{\sqrt{N}}(|w\rangle + \sqrt{N-1}|\alpha\rangle), \quad (12)$$

where

$$|\alpha\rangle \equiv \frac{1}{\sqrt{N-1}}{\sum_i}'|i\rangle \quad (13)$$

labels the state orthogonal to $|w\rangle$ corresponding to the superposition of all unmarked sites, and the prime on the sum denotes the exclusion of $i = w$. The linear part of the Hamiltonian is therefore a two-level operator in $|w\rangle$ and $|\alpha\rangle$. The equation of motion for any site $k \neq w$ takes the form $i\psi_k = -\gamma\sum_m \psi_m + g|\psi_k|^2\psi_k$, where $\psi_k \equiv \langle k|\psi\rangle$. Together with the fact that the initial amplitudes are the same at all sites, this means that the amplitudes at all unmarked sites are identical for all times. The nonlinear term can therefore be written

$$H_{\rm NL} = g|\psi_w|^2|w\rangle\langle w| + g|\psi_v|^2{\sum_i}'|i\rangle\langle i|, \quad (14)$$

where v denotes any vertex such that $v \neq w$. Because $\psi_\alpha = \sqrt{N-1}\psi_v$, the nonlinear term becomes

$$H_{\rm NL} = g|\psi_w|^2|w\rangle\langle w| + \frac{g|\psi_\alpha|^2}{N-1}\sum_i{}'|i\rangle\langle i|. \quad (15)$$

The equations of motion can be found using

$$\langle w|i\frac{\partial}{\partial t}|\psi\rangle = \langle w|H|\psi\rangle, \quad \langle\alpha|i\frac{\partial}{\partial t}|\psi\rangle = \langle\alpha|H|\psi\rangle. \quad (16)$$

After straightforward algebra, one obtains

$$i\frac{\partial}{\partial t}\psi_\alpha = -\gamma(N-1)\psi_\alpha - \gamma\sqrt{N-1}\psi_w + \frac{g}{N-1}|\psi_\alpha|^2\psi_\alpha, \quad (17a)$$

$$i\frac{\partial}{\partial t}\psi_w = -\gamma\sqrt{N-1}\psi_\alpha - (1+\gamma)\psi_w + g|\psi_w|^2\psi_w, \quad (17b)$$

with the initial state

$$\begin{pmatrix}\psi_\alpha(0)\\ \psi_w(0)\end{pmatrix} = \frac{1}{\sqrt{N}}\begin{pmatrix}\sqrt{N-1}\\ 1\end{pmatrix}. \quad (18)$$

As hoped, the equations of motion for the complete graph have now been reduced to a two-level operator. For a large search space ($N \gg 1$), Eqs. (17) become

$$i\frac{\partial}{\partial t}\psi_\alpha \approx -\gamma N\psi_\alpha - \gamma\sqrt{N}\psi_w + \frac{g}{N}|\psi_\alpha|^2\psi_\alpha, \quad (19a)$$

$$i\frac{\partial}{\partial t}\psi_w \approx -\gamma\sqrt{N}\psi_\alpha - (1+\gamma)\psi_w + g|\psi_w|^2\psi_w, \quad (19b)$$

with the initial state

$$\begin{pmatrix}\psi_\alpha(0)\\ \psi_w(0)\end{pmatrix} \approx \begin{pmatrix}1\\ 0\end{pmatrix}. \quad (20)$$

Since ψ_α and ψ_w are complex variables, they can be represented as

$$\psi_\alpha \equiv \sqrt{N_\alpha}e^{i\theta_\alpha}, \quad \psi_w \equiv \sqrt{N_w}e^{i\theta_w}, \quad (21)$$

where N_α and N_w are the populations of bosons in states $|\alpha\rangle$ and $|w\rangle$, respectively. Equations (19) then correspond to four coupled nonlinear differential equations. To reduce these to two coupled equations, one can define new variables:

$$\eta \equiv |\psi_w|^2 - |\psi_\alpha|^2 = N_w - N_\alpha; \quad (22a)$$

$$\phi \equiv \theta_w - \theta_\alpha, \quad (22b)$$

Equations (19) then become

$$\dot\eta = 2\gamma\sqrt{N}\sqrt{1-\eta^2}\sin(\phi), \quad (23a)$$

$$\dot\phi = \delta - \frac{g}{2}\eta - 2\gamma\sqrt{N}\frac{\eta}{\sqrt{1-\eta^2}}\cos(\phi), \quad (23b)$$

where δ is

$$\delta \equiv 1 - N\gamma - \frac{g}{2}. \quad (24)$$

Equations (23) are almost identical to those describing the Josephson dynamics of two weakly coupled BECs; see, for example, Eq. (2.6) in Ref. [60]. Note that taking the large-N limit is not necessary; the general-N case is recovered simply by replacing $N \to N-1$. The initial conditions for these variables are

$$(\eta(0),\phi(0)) = \left(-\frac{N-2}{N},0\right) = \left(-1+\frac{2}{N},0\right). \quad (25)$$

B. Complete search: $\delta = 0$

The complete search corresponds to the evolution of the state from the initial state, (18), where $\{|\psi_\alpha(0)|^2,|\psi_w(0)|^2\} = \{1-\frac{1}{N},\frac{1}{N}\}$, corresponding to the maximum probability of the superposition of all unmarked sites, to the state with maximum probability at the marked site, i.e., $\{|\psi_\alpha|^2,|\psi_w|^2\} = \{\frac{1}{N},1-\frac{1}{N}\}$. In other words, the search is complete when $|\eta(t_s)| = |\eta(0)|$. To determine if this is possible, it is convenient to interpret Eqs. (23) as Hamilton's equations of motion,

$$\dot\eta = -\frac{\partial H_C}{\partial\phi}, \quad \dot\phi = \frac{\partial H_C}{\partial\eta}, \quad (26)$$

for some classical Hamiltonian H_C. It is straightforward to verify that a Hamiltonian satisfying both Eq. (26) and Eq. (23) is

$$H_C = \delta\eta - \frac{g}{4}\eta^2 + 2\gamma\sqrt{N}\sqrt{1-\eta^2}\cos(\phi). \quad (27)$$

This has the same form as the classical Josephson Hamiltonian [61]. Since $\frac{\partial H}{\partial t} = 0$, this Hamiltonian is a constant of motion. The value of H_C for a trajectory starting at the initial point $\{\eta(0),\phi(0)\} = \{-1+\frac{2}{N},0\}$ must therefore be the same for the desired output $\{\eta(t_s),\phi(t_s)\} = \{1-\frac{2}{N},0\}$. This is only possible if $2\delta(1-\frac{2}{N}) = 0$ or $\delta = 0$, which corresponds to the homogeneous case. Setting $\delta = 0$ for a complete search specifies a critical value for γ:

$$\gamma^* = \frac{2-g}{2N}. \quad (28)$$

Note that the hopping coefficient must be positive, which requires $g < 2$.

1. *Fixed points*

The fixed points are obtained by setting Eqs. (23) to 0. These are

$$\phi_1 = 2m\pi, \quad m \in \mathbb{Z}; \quad \eta_0 = 0; \quad (29)$$

and

$$\phi_2 = (2m+1)\pi, \quad \begin{cases}\eta_+ = +\sqrt{1-\frac{4(g-2)^2}{g^2N}},\\ \eta_0 = 0,\\ \eta_- = -\sqrt{1-\frac{4(g-2)^2}{g^2N}}.\end{cases} \quad (30)$$

As shown in Fig. 1, η_+ and η_- approach 0 as g decreases and they both vanish at $g = g^*$, where

$$g^* = \frac{4}{2+\sqrt{N}}. \quad (31)$$

To make further progress, one must identify the nature of the fixed points; a brief review of these concepts is given in the Appendix. From Eqs. (23) with $\delta = 0$, the functions appearing in the Jacobian, (A5), are

$$a(\eta,\phi) = 2\gamma^*\sqrt{N}\sqrt{1-\eta^2}\sin(\phi), \quad (32a)$$

$$b(\eta,\phi) = -\frac{g}{2}\eta - 2\gamma^*\sqrt{N}\frac{\eta}{\sqrt{1-\eta^2}}\cos(\phi). \quad (32b)$$

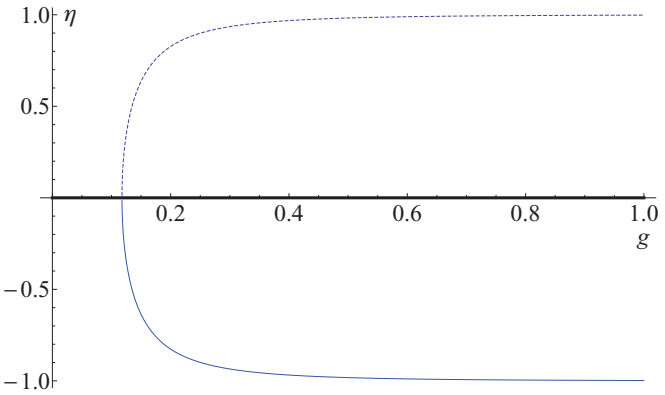

FIG. 1. (Color online) Second set of fixed points as a function of g for $N = 1024$. The dashed line represents η_+; the solid line, η_-; and the thick horizontal line, η_0.

The Jacobian is therefore

$$J = \frac{2\gamma^*\sqrt{N}}{\sqrt{1-\eta^2}} \begin{pmatrix} -\eta\sin(\phi) & (1-\eta^2)\cos(\phi) \\ -\frac{g\sqrt{1-\eta^2}}{4\gamma^*\sqrt{N}} - \frac{\cos(\phi)}{1-\eta^2} & \eta\sin(\phi) \end{pmatrix}. \quad (33)$$

For the first set of fixed points $(\eta,\phi) = (0,2m\pi)$, the Jacobian matrix becomes

$$J_{(0,2m\pi)} = \begin{pmatrix} 0 & \frac{2-g}{\sqrt{N}} \\ -\frac{g}{2} - \frac{2-g}{\sqrt{N}} & 0 \end{pmatrix}, \quad (34)$$

where the condition $\gamma^* = (2-g)/2N$ has been applied. The eigenvalues are

$$\lambda_\pm = \pm i\sqrt{\frac{(2-g)[4+g(\sqrt{N}-2)]}{2N}}. \quad (35)$$

Because $N \gg 1$ and $\gamma^* > 0$, the eigenvalues are strictly imaginary. The fixed points are therefore marginally stable, or centers. The orbit in the vicinity of the fixed point at $(\eta,\phi) = (0,0)$ is counterclockwise, as shown in the center (black) filled and dashed circles in Fig. 2.

The second set of fixed points corresponds to $(\eta,\phi) = (\{\eta_\pm,0\},(2m+1)\pi)$. Consider first the case $(\eta,\phi) = (0,(2m+1)\pi)$. The eigenvalues of the Jacobian matrix are then

$$\lambda_\pm = \pm\sqrt{\frac{(2-g)[-4+g(\sqrt{N}+2)]}{2N}}. \quad (36)$$

If $g > \frac{4}{2+\sqrt{N}}$, these eigenvalues are both real. One is negative and the other positive, yielding an unstable saddle fixed point. The trajectories in the vicinity of these fixed points are depicted as (dark-blue) vectors in Fig. 3. If $g < \frac{4}{2+\sqrt{N}}$, then both eigenvalues are imaginary, yielding a marginally stable fixed point or center. The orbits in the vicinity of the fixed points $(\eta,\phi) = (0, \pm\pi)$ are clockwise, as shown iby the center (black) filled and dashed circles in Fig. 2.

Consider next the fixed points $(\eta,\phi) = (\eta_\pm,(2m+1)\pi)$. For both cases, the eigenvalues of the Jacobian matrix are

$$\lambda_\pm = \pm\frac{1}{2}\sqrt{\frac{4(2-g)^2}{N} - g^2}. \quad (37)$$

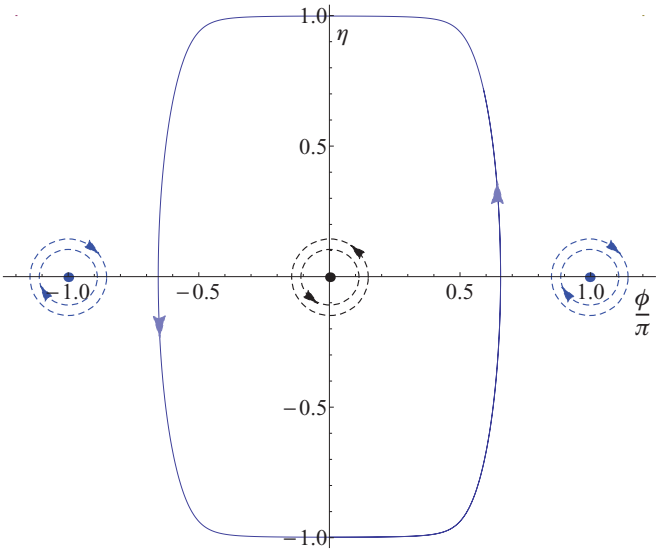

FIG. 2. (Color online) Trajectory in phase space for $N = 1024$, $g = g^*$, $\gamma = \gamma^* = \frac{2-g^*}{2N}$. The center (black) and left and right (dark blue) filled circles are marginally stable fixed points $(\eta,\phi) = (0,0)$ and $(0, \pm\pi)$, respectively. Dashed circles are the orbits around these fixed points. The (light-blue) curve corresponds to the trajectory taken for a complete search.

For $g < \frac{4}{2+\sqrt{N}}$ the solutions $\eta_\pm$ do not exist. For $g > \frac{4}{2+\sqrt{N}}$, both eigenvalues become imaginary, yielding a marginally stable fixed point or center. The only difference between the two cases is that trajectories near the η_+ flow counterclockwise, opposite to the clockwise direction for those near η_-; these are shown as the top (green) and bottom (red) rows of three orbits in Fig. 3.

Figure 2 clearly shows that all of the fixed points in the $g \lesssim g^*$ regime are marginally stable or centers. Hence in this regime the trajectory starts from the initial point $(\eta(0),\phi(0)) = (-1+\frac{2}{N},0)$, rotates around the origin, and reaches the final point of the search $(\eta(t_s),\phi(t_s)) = (1-\frac{2}{N},0)$. This behavior is depicted as the light-blue curve in Fig. 2. Thus, a complete search is attainable in this regime.

In the other regime $g > g^*$ there is a saddle fixed point $(\eta,\phi) = (\eta_-,\pi)$ near the initial point $(-1,0)$. The trajectory

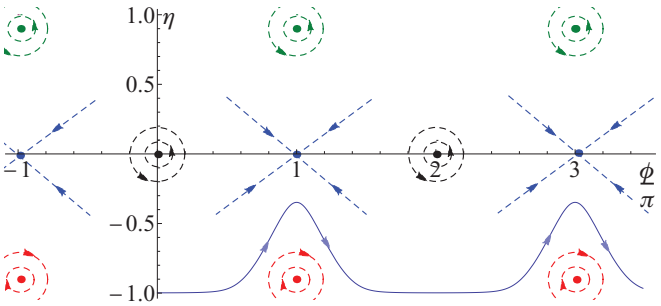

FIG. 3. (Color online) Trajectory in phase space with $N = 1024$, $g = 2g^*$, and $\gamma = \gamma^* = (2-g^*)/2N$ [lower (light-blue) curve]. The bottom row of three (red) filled circles represents η_-; the top row of three (green) filled circles, η_+; and the middle row of two (black) filled circles, η_0. The (dark-blue) vectors are the eigenvectors of the Jacobian matrix at $(0,(2m+1)\pi)$.

will continue along the positive ϕ and η will remain close to η_-, so that it would never reach $\eta = +1$. As shown in Fig. 3, it is not likely to have a complete search in this regime. In principle, one might still have a complete search for $g \gtrsim g^*$ because the linearization procedure is strictly valid only right at the fixed points, but the range would likely not be extensive. In any case, for any $g \in [0, g^*]$ a complete search is attainable. The value $g = g^*$ is chosen for the remainder of the calculations.

2. Search time

Now that the nonlinear quantum search of the complete graph has been shown to be successful for a range of interaction strengths g, it is important to determine the scaling of the search time t_s with the number of sites for large N. As shown in Fig. 2, the trajectory closely resembles a rectangle. Consider the dynamical equations, (23), with $\delta = 0$ and the large-N values of $g = g^* \approx 4/\sqrt{N}$ and $\gamma = \gamma^* = (2-g)/2N \approx 1/N$:

$$\dot{\eta} = \frac{2}{\sqrt{N}}\sqrt{1-\eta^2}\sin(\phi), \tag{38a}$$

$$\dot{\phi} = -\frac{2}{\sqrt{N}}\eta\left[1 + \frac{1}{\sqrt{1-\eta^2}}\cos(\phi)\right]. \tag{38b}$$

For $N \gg 1$, the right-hand sides of Eq. (38) approach 0, and the trajectories are approximated by $\eta(t) \approx k_1$ and $\phi \approx k_2$, with k_1 and k_2 constants. These can be approximately decomposed into the following steps.

(I) Constant η: The initial point, $(\eta,\phi) \approx (-1,0) \to (-1,\phi_c)$, where ϕ_c is the intersection of the trajectory with the ϕ axis.

(II) Constant ϕ: $(\eta,\phi) \approx (-1,\phi_c) \to (1,\phi_c)$.

(III) Constant η: $(\eta,\phi) \approx (1,\phi_c) \to (1,0)$.

The search time t_s can be written as

$$t_s = \int_{(\mathrm{I})} dt + \int_{(\mathrm{II})} dt + \int_{(\mathrm{III})} dt. \tag{39}$$

For the first and third steps η is approximately constant, just as ϕ is approximately constant for the second step, so

$$t_s \approx \int_0^{\phi_c} \frac{d\phi}{\dot{\phi}} + \int_{-1}^{1} \frac{d\eta}{\dot{\eta}} + \int_{\phi_c}^{0} \frac{d\phi}{\dot{\phi}}. \tag{40}$$

The initial condition, (25), gives a trajectory $\eta(t) \approx -1$ and $\dot{\phi} \to \infty$ so that the first and third integrals make an insignificant contribution to t_s. As shown in Fig. 4, the $\eta \approx k_1$ transition $\phi = 0 \to \phi_c$ is much faster than the $\phi \approx k_2$ transition $\eta = -1 \to 1$ (during which the phase hovers in the vicinity of ϕ_c). This system is an example of a relaxation oscillator [62]. Therefore one can express t_s as

$$t_s \approx \int_{-1}^{1} \frac{d\eta}{\dot{\eta}} \approx \frac{\sqrt{N}}{2\sin(\phi_c)} \int_{-1}^{1} \frac{d\eta}{\sqrt{1-\eta^2}} = \frac{\pi}{2}\left(\frac{1}{\sin(\phi_c)}\right)\sqrt{N} \tag{41}$$

for large N. Besides the factor of $1/\sin(\phi_c)$, this is the usual expression for the spatial search time.

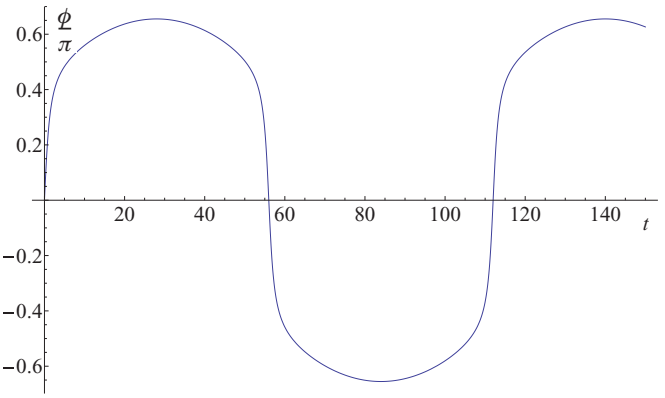

FIG. 4. (Color online) Phase ϕ as a function of time, when $\delta = 0$, $g = g^* = \frac{4}{\sqrt{N}}$, and $N = 1024$.

Setting $\delta = 0$, $g = g^*$, and $\gamma = \gamma^*$, the classical Hamiltonian H_C in Eq. (27) takes the form

$$H_C = \frac{2\sqrt{1-\eta^2}\cos(\phi) - \eta^2}{2+\sqrt{N}}. \tag{42}$$

For the initial condition $\eta(0) = -1 + \frac{2}{N} \approx -1$ for $N \gg 1$, the classical Hamiltonian becomes $H_C \approx -\frac{1}{\sqrt{N}}$ and this value is preserved during the evolution. When the trajectory depicted in Fig. 2 crosses the ϕ axis at the point $(\eta,\phi) = (0,\phi_c)$, the Hamiltonian is approximately $H_C \approx 2\cos(\phi_c)/\sqrt{N}$. The value of the phase at this point is therefore $\phi_c = \cos^{-1}(-1/2) = 2\pi/3$. This is consistent with the time evolution of the phase shown in Fig. 4. The time for the nonlinear search in the large-N limit, Eq. (41), is therefore

$$t_s = \frac{\pi}{2}\frac{2}{\sqrt{3}}\sqrt{N} = \frac{\pi}{\sqrt{3}}\sqrt{N}, \tag{43}$$

slower than the linear search by a constant factor of $2/\sqrt{3} \approx 1.155$.

It is important to check that the linear search time is recovered in the case $g \to 0$. In this case one has $\gamma^* = 1/N$ (valid for all N). The trajectories will then cross the η axis at the initial condition $(\eta(0),\phi(0)) = (-1+\frac{2}{N},0)$ when the classical Hamiltonian, (27), takes the value $H_C \approx \frac{2\sqrt{2}}{N}$, valid for $N \gg 1$. When the trajectory crosses the ϕ axis at $(\eta,\phi) = (0,\phi_c)$, the classical Hamiltonian becomes $H_C = \frac{2}{\sqrt{N}}\cos(\phi_c)$. Because the Hamiltonian is a constant of the motion, one obtains $\phi_c \approx \cos^{-1}(\sqrt{\frac{2}{N}}) \approx \pi/2$. The search time for the linear problem, Eq. (41), is then $t_s = (\pi/2)\sqrt{N}$, consistent with expectations.

3. Errors

In the foregoing analysis, it has been assumed that the initial amplitudes at all sites are always identical, as are the amplitudes to hop from site to site. The derivation of the nonlinear Hamiltonian, (14), is only valid under these conditions. Relaxing these assumptions prevents the reduction of the N-vertex system to a two-dimensional problem. Instead, one must solve N simultaneous coupled nonlinear differential

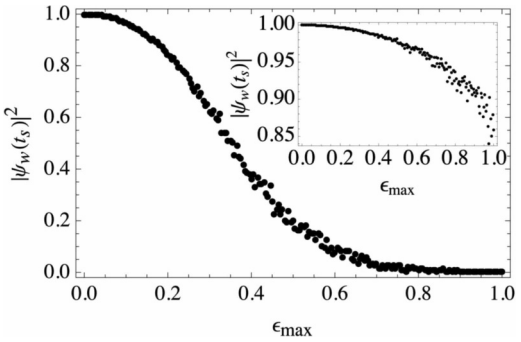

FIG. 5. Probability of obtaining the marked site $|\psi_w(t_s)|^2$ at the search time $t_s = \pi\sqrt{N/3}$ as a function of the maximum error $\epsilon_{\max}$ in the initial state, (45), for $g = 4/\sqrt{N}$, $\gamma_{ij} = \gamma^* = (2-g)/2N$, and $N = 600$. Inset: Success probability under the same conditions but assuming that the initial state has a constant phase.

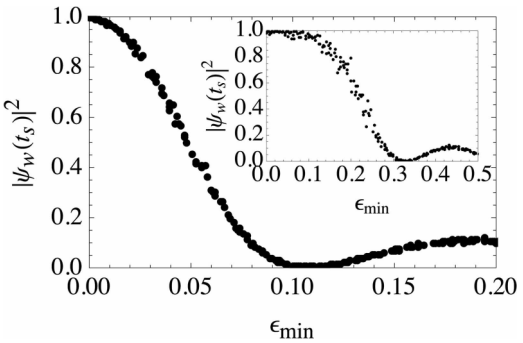

FIG. 6. Probability of obtaining the marked site $|\psi_w(t_s)|^2$ at the search time $t_s = \pi\sqrt{N/3}$ as a function of the number of zero-weight edges $\epsilon_{\min}$, assuming a uniform initial state, $g = 4/\sqrt{N}$, $\gamma_{ij} = \gamma^* = (2-g)/2N$ for nonzero edges, and $N = 300$. Inset: Success probability under the same conditions but assuming that the nonzero edges now have random amplitudes $\gamma_{ij} > 2\gamma^*\epsilon_{\min}$.

equations of the form

$$i\frac{\partial}{\partial t}\psi_j = -\sum_{k=1}^{N}\gamma_{jk}\psi_k - \psi_w\delta_{jw} + g|\psi_j|^2\psi_j, \qquad (44)$$

where $j = 1,\ldots,N$ including the marked site $j = w$.

Consider first the possibility that the initial state is not the uniform superposition of all sites but, instead, some arbitrary input. Let the initial state be

$$|\psi(0)\rangle = \frac{1}{\sqrt{N+\sum_j \epsilon_j}}\sum_{j=1}^{N}\sqrt{1+\epsilon_j}e^{i\pi\epsilon_j}|j\rangle, \qquad (45)$$

where the uniform amplitudes of Eq. (3) at each site have now been deformed by a random real number $|\epsilon_j| \leqslant \epsilon_{\max}$ as well as phases in the range $\{-\epsilon_{\max}\pi,\epsilon_{\max}\pi\}$. Equations (44) were solved numerically in Mathematica with $g = g^* = 4/\sqrt{N}$, $\gamma_{ij} = \gamma^* = (2-g)/2N$, and $t = t_s = \pi\sqrt{N/3}$, and the resulting probability of finding the marked site $|\psi_w(t_s)|^2$ is plotted in Fig. 5 for the particular case $N = 600$. While the data show some fluctuations due to the randomization, the results clearly indicate that the marked site can be found with a probability exceeding 90% for errors $\epsilon_{\max} \lesssim 0.15$. Surprisingly, if the initial state is assumed to possess phase coherence (i.e., no randomized phases are included), then the marked site can be obtained with a probability exceeding 90% for $\epsilon_{\max} \lesssim 0.8$, as shown in the inset in Fig. 5. Note that the $\epsilon_{\max} = 1.0$ case corresponds to a completely random (but constant-phase) initial state. These results indicate that the nonlinear quantum search is robust against initialization noise.

Consider second the possibility that the hopping amplitudes γ_{ij} can vary while the initial state is assumed to be uniform. The simplest case is to consider the effect of randomly deleting edges, i.e., to suppose that $\gamma_{ij} = \gamma^*$ for some fraction $1-\epsilon_{\min}$ of the edges and is 0 otherwise. Given a random variable $\epsilon_{ij} \in \{0,1\}$, then one can define

$$\gamma_{ij} = \begin{cases}\gamma^* & \text{if} \quad \epsilon_{ij} > \epsilon_{\min},\\ 0 & \text{otherwise,}\end{cases} \qquad (46)$$

which produces an Erdös-Rényi random graph [58] with approximately $(1-\epsilon_{\min})\,N(N-1)/2$ edges. Figure 6 depicts the results for $g = g^* = 4/\sqrt{N}$ and $N = 300$, assuming a uniform initial condition. The data show that the quantum search success probability drops precipitously as a function of the fraction of 0 edges $\epsilon_{\min}$; to ensure 90% or better probability at the marked site requires $\epsilon_{\min} \lesssim 0.02$. The output probability does not decrease monotonically with $\epsilon_{\min}$ but, in fact, increases again slightly as the number of zero-weight edges increases beyond approximately 10%. Similar observations of enhanced quantum search with increased connectivity have been reported in the context of the linear discrete-time quantum walk [59].

Another model for including error in the structure of the graph is to assume that the values of the hopping amplitudes are not constant. Consider for concreteness the case $\gamma_{ij} = (1+\epsilon_{ij})\gamma^*$ with the random variable $|\epsilon_{ij}| \leqslant 1$. The numerics yield the surprising result that the probability of finding the marked site $|\psi_w(t_s)|^2 \to 1$ as $N \to \infty$ (not shown). For large graphs, the success of the algorithm is therefore not affected by the randomization of the hopping amplitudes, as long as their average is γ^* and the initial state is assumed to be uniform. To make contact with the results in Erdös-Rényi graphs, suppose that, in addition to the randomization of the hopping amplitudes, one adds the supplementary condition that $\gamma_{ij} = 0$ if $1+\epsilon_{ij} < 2\epsilon_{\min}$ (recall that $0 \leqslant \gamma_{ij} \leqslant 2\gamma^*$). In this case $\epsilon_{\min}$ again reflects the fraction of edges that have zero weight, while the remaining edges have random amplitudes $\gamma_{ij} > 2\gamma^*\epsilon_{\min}$. The results, depicted in the inset in Fig. 6, indicate that randomizing the hopping amplitudes in this way in fact improves the algorithm's success probability under edge deletion relative to the unweighted case. Under these conditions, an output probability exceeding 90% can be obtained with approximately 12% of the complete graph's edges deleted, compared with only approximately 2% in the unweighted case.

C. Incomplete search: $\delta \neq 0$

As discussed at the beginning of Sec. III B, a complete search is equivalent to finding a trajectory that makes the transition $\eta = -1 + \frac{2}{N} \to 1 - \frac{2}{N}$ possible. Because H_C is a constant of the motion, however, a complete search requires

$\delta = 0$. That said, it is conceivable that setting $\delta \neq 0$ could yield a time t_s where the relative occupation of the marked site would instead be $\eta \lesssim 1 - \frac{2}{N}$. Consider again the fixed points of Eqs. (23). Evidently $\phi = m\pi$ ensures that the right-hand side of Eq. (23a) is 0, but $\eta = 0$ no longer accomplishes this for the right-hand side of Eq. (23b) because $\delta = 1 - N\gamma - g/2 \neq 0$ by assumption. Now that the search cannot be complete, it is not necessary to keep the exact expressions for finite N, and one can work entirely in the limit $N \gg 1$. If one again sets $\gamma = \gamma^* = 1/N$, then $\delta = -g/2$. Choosing $g = \alpha/N^\beta$, where α and β are both positive real numbers, gives $\delta \sim N^{-\beta}$, which vanishes for large N. Equations (23) then become

$$\dot{\eta} = \frac{2\sqrt{1-\eta^2}}{\sqrt{N}} \sin(\phi), \tag{47a}$$

$$\dot{\phi} = -\frac{\alpha(1+\eta)}{2N^\beta} - \frac{2\eta}{\sqrt{N}\sqrt{1-\eta^2}} \cos(\phi). \tag{47b}$$

To determine the maximum value reached by η, consider the classical Hamiltonian, (27), which now has the form

$$H_C = -\frac{\alpha\eta(2+\eta)}{4N^\beta} + \frac{2\sqrt{1-\eta^2}}{\sqrt{N}} \cos(\phi). \tag{48}$$

At the initial conditon $(\eta,\phi) \approx (-1,0)$, the classical Hamiltonian is $H_C(0) = \alpha/4N^\beta$, which is a constant of the motion. Note that for the incomplete search, the classical Hamiltonian is now positive. The accessible values of (η,ϕ) are found by setting $H_C = H_C(0)$. The N dependence disappears if $\beta = 1/2$ (i.e., $g = \alpha/\sqrt{N}$), and the only two real solutions correspond to $\eta_1 = -1$ and

$$\eta_2 = -1 + \frac{4(3x)^{1/3}}{3\alpha^2} - \frac{16\cos^2(\phi)}{(3x)^{1/3}}, \tag{49}$$

where

$$x = \alpha^3 \cos^2(\phi)\sqrt{3}\sqrt{27\alpha^2 + 64\cos^2(\phi)} + 9\alpha^4 \cos^2(\phi). \tag{50}$$

Though the solution, (49), is a bit unwieldy, a few observations can immediately be made. For small and large α, one obtains, respectively,

$$\eta_2(\alpha \ll 1) \approx 1 - \frac{\alpha^2}{8} \sec^2(\phi); \tag{51}$$

$$\eta_2(\alpha \gg 1) \approx -1 + 4\left(\frac{2\cos^2(\phi)}{\alpha^2}\right)^{1/3}. \tag{52}$$

Note that only even powers of α appear in these expansions, indicating that the dynamics is unaffected by the sign of the nonlinearity. Equation (51) shows that a complete search is only possible for the noninteracting case $\alpha = 0$, which is consistent with $\delta = 0$. For any finite interaction strength in this $\delta \neq 0$ regime, a complete search is not possible. The relative fraction at the marked site decreases with α, and Eq. (52) reveals that it is asymptotically 0 for very large nonlinearities (though one still requires $g < 2$). Physically, the large interaction between atoms favors the initial state which is the superposition of occupying all sites in the graph. This is the dynamical self-trapping which has been noted previously for interacting BECs [63,64].

Interestingly, $\eta_2^{(\max)}$ is independent of the size of the search problem (keep in mind, however, that $g = \alpha/\sqrt{N}$ so that the strength of the nonlinearity decreases with N). Note also that the maximum probability is reached for $\phi = 0$. For example, $\eta_2^{(\max)} = 0.99$ requires $\alpha \approx 0.28$. The case $\eta_2 = 0$ can be obtained directly from Eq. (49), and one obtains $\alpha = \pm 8\cos(\phi)$. At this value of α, the probability of occupying the marked site is exactly $1/2$; for any smaller α it is higher.

It remains to calculate the time for the incomplete search t_s. As in the $\delta = 0$ case, the right-hand sides of Eqs. (47) approach 0, which means that the trajectories are approximated by constant lines. Again, the ϕ evolution is much faster than the η evolution for the $\eta \approx \eta_1 = -1$ trajectory. The $\eta \approx \eta_2$ trajectory is not going to be as fast because the $\sqrt{1-\eta_2}$ term in Eq. (47b) is no longer almost 0. The search time is then approximately

$$t_s \approx \int_{-1}^{1} \frac{d\eta}{\dot{\eta}} + \int_{\phi_c}^{0} \frac{d\phi}{\dot{\phi}} = \frac{\pi\sqrt{N}}{2\sin(\phi_c)} + \int_{\phi_c}^{0} \frac{d\phi\sqrt{N}}{-\frac{\alpha(1+\eta)}{2} - \frac{2\eta}{\sqrt{1-\eta^2}}\cos(\phi)}. \tag{53}$$

The critical angle ϕ_c is obtained by equating the classical Hamiltonian, (48), for $(\eta,\phi) = (0,\phi_c)$ with $H_C(0)$; this gives $\alpha/4\sqrt{N} = 2\cos(\phi_c)/\sqrt{N}$ or

$$\phi_c = \cos^{-1}\left(\frac{\alpha}{8}\right) \approx \frac{\pi}{2} - \frac{\alpha}{8} \tag{54}$$

for small α. For the linear case ($\alpha = 0$), the critical angle coincides with that found in the previous section for the complete search. The first term in Eq. (53) is therefore $\pi\sqrt{N}/2\sin(\phi_c) \approx (\pi\sqrt{N}/2)/\sqrt{1-\alpha^2/64}$, which restricts the strength of the nonlinearity to $|\alpha| < 8$ (recall that for $|\alpha| > 8$ the probability at the marked site is $< \frac{1}{2}$).

The second term can be simplified by assuming that the value of η, given in Eq. (49), remains approximately constant over the range of integration $\{-\phi_c,0\}$. In fact, plotting η for a range of α shows that it varies from 0 to its maximum value, Eq. (51), but this increase occurs only over a very small region in the vicinity of $\phi = \phi_c$. For small α, the time for the incomplete search, given by Eq. (53), can be approximated as

$$t_s \approx \frac{\pi}{2}\sqrt{N}\left(1 + \frac{\alpha^2}{128}\right) - \sqrt{N}\int_{-\phi_c}^{0} \frac{d\phi}{\alpha + 4\cos(\phi)/\alpha} \approx \frac{\pi}{2}\sqrt{N}\left[1 + \frac{\alpha}{2\pi}\ln\left(\frac{\alpha}{16}\right) + \frac{\alpha^2}{128}\right]. \tag{55}$$

Because the α-dependent correction terms are negative in the regime $0 < \alpha < 8$, the time for the incomplete search is generally shorter than that for the complete search by a small factor dependent on the strength of the nonlinearity.

IV. CONCLUSIONS

In this work we considered the spatial search algorithm on a lattice with the topology of the complete graph, under the assumption that the continuous-time quantum walk is effected by a zero-temperature BEC. In the mean-field approximation, the equations of motion become nonlinear and correspond to the discrete GP equation. The analytical results, using methods in nonlinear dynamics and numerical calculations, indicate that

a complete spatial search remains possible even in the presence of nonlinearity.

For a successful search, the nonlinear coupling constant must decrease with the system size as $N^{-1/2}$ and the intersite hopping amplitude decreases as N^{-1}, where N is the number of sites. The latter condition coincides with the criterion for a complete search found for the linear search problem in the complete graph [21]. Under these circumstances, the search time is found to scale as $t_s \propto \sqrt{N}$, with an overall constant factor that depends weakly on the strength of the nonlinearity. The probability of success generically decreases with the strength of the nonlinearity, but there are particular choices of parameters where the success probability can be made unity in the limit of large N. The numerical results further indicate that random errors in the input state amplitudes and the hopping amplitudes are not deleterious for the performance of the algorithm but that the inclusion of phase errors in the input state or edge deletions quickly erode the probability of finding the marked site. Overall, the quantum search is found to be robust to error under a variety of conditions. It would be interesting to explore the influence of nonunitary (thermal) noise on the performance of the nonlinear search. In the limit of zero nonlinearity, the present results in the absence of error completely recover those of Ref. [21].

The dynamics of the nonlinear system agree closely with those of the linear quantum walk. This indicates that nonlinearity, as long as its strength is kept bounded for a given system size, is no impediment to the implementation of a quantum spatial search. The results suggest that BECs consisting of huge numbers of particles could be candidates for the implementation of useful quantum algorithms. The hopping amplitude and the strength of the nonlinearity need to be adjusted for a given size of the search space. In ultracold atomic gases, for example, in principle the former could be accomplished by adjusting the depth or spacing of a lattice [34], and the latter through the use of Feshbach resonances [65], though constructing a lattice with the connectivity of the complete graph is not currently feasible in these systems.

It would be preferable in practice to conduct the spatial search on a regular lattice, for example, a square lattice in three or lower dimensions. Unfortunately, continuous-time quantum walks based on the ordinary discrete Schrödinger equation do not provide useful quantum speedups on these lattices over the classical search time, though discrete-time quantum walks that do can be constructed [18]. That said, if the particle dispersion relation is linear rather than quadratic, full quantum speedup is achievable on a three-dimensional square lattice [22]. One practical strategy to achieve this is to artificially induce Dirac fermions by suitably preparing an optical lattice [66]. More directly, the excitations of a zero-temperature weakly interacting BEC on a lattice are characterized by a linear dispersion relation, which is a hallmark of the underlying superfluidity in these systems [49]. It is therefore conceivable that the nonlinear mean-field dynamics of the BEC on a cubic lattice would yield the full quantum speedup for the continuous-time spatial search problem. This possibility will be explored in future work.

Note added in proof. Recently we became aware of another work that investigates the system addressed in the present study [67]. While the results are consistent with ours when there is overlap, in that work the strength of the nonlinear coupling is assumed to vary with time. Their methods and conclusions are therefore complementary to ours.

ACKNOWLEDGMENTS

The authors are grateful to David Meyer for originally stimulating this line of inquiry and for productive conversations, and to Jörn Davidsen, Dennis Salahub, and Thomas Wong for their comments on preliminary manuscripts. This work was supported by the Natural Sciences and Engineering Research Council of Canada.

APPENDIX: CHARACTERIZING FIXED POINTS

This discussion follows Ref. [62]. Consider a general two-dimensional nonlinear system of equations:

$$\dot{u} = a(u,v), \quad \dot{v} = b(u,v).$$

A fixed point or equilibrium point is defined by

$$\dot{w} \equiv \begin{pmatrix} \dot{u} \\ \dot{v} \end{pmatrix} \equiv 0. \tag{A1}$$

Suppose (u^*,v^*) is a fixed point for this system, satisfying $a(u^*,v^*) = b(u^*,v^*) = 0$. Let $u' = u - u^*$ and $v' = v - v^*$. For small u' and v'

$$\dot{u'} \approx a(u^*,v^*) + \frac{\partial a}{\partial u}(u^*,v^*)u' + \frac{\partial a}{\partial v}(u^*,v^*)v'; \tag{A2a}$$

$$\dot{v'} \approx b(u^*,v^*) + \frac{\partial b}{\partial u}(u^*,v^*)u' + \frac{\partial b}{\partial v}(u^*,v^*)v'. \tag{A2b}$$

Since (u^*,v^*) is a fixed point, $a(u^*,v^*) = b(u^*,v^*) = 0$. Close to the fixed points ($u' \ll 1, v' \ll 1$), Eqs. (A2) can be written as

$$\dot{w'} \approx J w', \tag{A3}$$

where

$$w' = \begin{pmatrix} u' \\ v' \end{pmatrix}, \tag{A4}$$

and J is the Jacobian matrix

$$J = \begin{pmatrix} \frac{\partial a}{\partial u} & \frac{\partial a}{\partial v} \\ \frac{\partial b}{\partial u} & \frac{\partial b}{\partial v} \end{pmatrix}_{(u^*,v^*)}. \tag{A5}$$

The general solution of Eq. (A3) when J is nondegenerate and invertible is

$$w(t) = c_1 z_1 e^{\lambda_1 t} + c_2 z_2 e^{\lambda_2 t}, \tag{A6}$$

where λ_i and z_i are the eigenvalues and eigenvectors of the Jacobian matrix J, respectively; c_1 and c_2 are constants which are determined by the initial conditions. There are four possibilities for the stability of the fixed points.

(1) λ_1 and λ_2 both real:

(a) *Stable fixed point*. If $\lambda_1 < 0$ and $\lambda_2 < 0$, then $w' \to 0$ as $t \to \infty$.

(b) *Unstable fixed point*. If $\lambda_1 > 0$ and $\lambda_2 > 0$, then $w' \to \infty$ as $t \to \infty$.

(c) *Unstable saddle point*. If $\lambda_1 < 0 < \lambda_2$, then if $w'(0)$ is a multiple of z_1, $w' \to 0$ as $t \to \infty$ (stable along the direction

of z_1); alternatively, if $w'(0)$ is a multiple of z_2, then $w' \to \infty$ as $t \to \infty$ (unstable along the direction of z_2).

Marginally stable fixed point or center: λ_1 and λ_2 are both complex. If $\mathrm{Re}(\lambda_i) = 0$, then $|w'| \to$ const. as $t \to \infty$. Trajectories circulate around the fixed point and eventually return to the initial point; these are closed orbits.

The Hartman-Grobman theorem states that the dynamics of the linearized system in the vicinity of hyperbolic fixed points, where $\mathrm{Re}(\lambda_i) \neq 0$, will be similar to that of the original nonlinear system. If one or both eigenvalues do not satisfy this condition, the fixed point is nonhyperbolic and therefore the dynamics are fragile to the inclusion of nonlinearity. That said, suppose that (u^*, v^*) is an isolated fixed point that is marginally stable, and there exists a conserved quantity $H_C(u,v)$. If (u^*, v^*) is a local minimum of $H_C(u,v)$, then all trajectories sufficiently close to (u^*, v^*) are closed.

[1] L. K. Grover, *Proceedings of the 28th Annual ACM STOC* (Association for Computing Machinery, New York, NY, 1996), p. 212.
[2] L. K. Grover, Phys. Rev. Lett. **79**, 325 (1997).
[3] C. H. Bennett, E. Bernstein, G. Brassard, and U. Vazirani, SIAM J. Comput. **26**, 1510 (1997).
[4] D. A. Meyer, J. Stat. Phys. **85**, 551 (1996).
[5] D. A. Meyer, Phys. Lett. A **223**, 337 (1996).
[6] J. Watrous, J. Comput. Syst. Sci. **62**, 376 (2001).
[7] A. Ambainis *et al.*, *Proceedings of the 33rd Annual ACM STOC* (Association for Computing Machinery, New York, NY, 2001), p. 37.
[8] D. Aharonov, A. Ambainis, J. Kempe, and U. Vazirani, *Proceedings of the 33rd Annual ACM STOC* (Association for Computing Machinery, New York, NY, 2001), p. 50.
[9] E. Farhi and S. Gutmann, Phys. Rev. A **58**, 915 (1998).
[10] A. Childs, E. Farhi, and S. Gutmann, Quant. Inf. Proc. **1**, 35 (2002).
[11] J. Kempe, Contemp. Phys. **44**, 307 (2003).
[12] A. Ambainis, Int. J. Quant. Inf. **1**, 507 (2003).
[13] V. Kendon, Phil. Trans. R. Soc. A **364**, 3407 (2006).
[14] D. Reitzner, D. Nagaj, and V. Bužek, Acta Physica Slovaca **61**, 603 (2011).
[15] S. E. Venegas-Andraca, Quant. Inf. Proc. **11**, 1015 (2012).
[16] N. Shenvi, J. Kempe, and K. B. Whaley, Phys. Rev. A **67**, 052307 (2003).
[17] M. Szegedy, *Proceedings of the 45th IEEE Symposium on Foundations of Computer Science* (IEEE Computer Society, Washington, DC, 2004), p. 32.
[18] A. Ambainis, J. Kempe, and A. Rivosh, *Proceedings of the 16th ACM-SIAM Symposium on Discrete Algorithms* (Society for Industrial and Applied Mathematics, Philadelphia, PA, 2005), p. 1099.
[19] M. Santha, *Proceedings of the Fifth International Conference on Theory and Applications of Models of Computation, TAMC 2008, Xi'an, China, 2008*, edited by M. Agrawal, D.-Z. Du, Z. Duan, and A. Li, Lecture Notes in Computer Science (Springer, Berlin, Heidelberg, 2008), p. 31.
[20] D. Reitzner, M. Hillery, E. Feldman, and V. Bužek, Phys. Rev. A **79**, 012323 (2009).
[21] A. M. Childs and J. Goldstone, Phys. Rev. A **70**, 022314 (2004).
[22] A. M. Childs and J. Goldstone, Phys. Rev. A **70**, 042312 (2004).
[23] E. Agliari, A. Blumen, and O. Mülken, Phys. Rev. A **82**, 012305 (2010).
[24] F. Magniez, A. Nayak, J. Roland, and M. Santha, SIAM J. Comput. **40**, 142 (2011).
[25] A. Tulsi, Phys. Rev. A **78**, 012310 (2008).
[26] N. B. Lovett *et al.*, Nat. Comput. **11**, 23 (2012).
[27] J. Du *et al.*, Phys. Rev. A **67**, 042316 (2003).
[28] C. A. Ryan, M. Laforest, J. C. Boileau, and R. Laflamme, Phys. Rev. A **72**, 062317 (2005).
[29] H. Schmitz *et al.*, Phys. Rev. Lett. **103**, 090504 (2009).
[30] F. Zähringer *et al.*, Phys. Rev. Lett. **104**, 100503 (2010).
[31] A. Schreiber *et al.*, Phys. Rev. Lett. **104**, 050502 (2010).
[32] M. A. Broome *et al.*, Phys. Rev. Lett. **104**, 153602 (2010).
[33] M. Karski *et al.*, Science **325**, 174 (2009).
[34] I. Bloch, J. Dalibard, and W. Zwerger, Rev. Mod. Phys. **80**, 885 (2008).
[35] H. B. Perets *et al.*, Phys. Rev. Lett. **100**, 170506 (2008).
[36] A. Peruzzo *et al.*, Science **329**, 1500 (2010).
[37] Y. Bromberg, Y. Lahini, R. Morandotti, and Y. Silberberg, Phys. Rev. Lett. **102**, 253904 (2009).
[38] J. O. Owens *et al.*, New J. Phys. **13**, 075003 (2011).
[39] J. D. A. Meinecke *et al.*, Phys. Rev. A **88**, 012308 (2013).
[40] A. Crespi *et al.*, Nature Photonics **7**, 322 (2013).
[41] A. Schreiber *et al.*, Science **336**, 55 (2012).
[42] O. Mandel, M. Greiner, A. Widera, T. Rom, T. W. Hänsch, and I. Bloch, Phys. Rev. Lett. **91**, 010407 (2003).
[43] M. A. Broome *et al.*, Science **339**, 794 (2013).
[44] J. B. Spring *et al.*, Science **339**, 798 (2013).
[45] J. K. Gamble, M. Friesen, D. Zhou, R. Joynt, and S. N. Coppersmith, Phys. Rev. A **81**, 052313 (2010).
[46] S. D. Berry and J. B. Wang, Phys. Rev. A **83**, 042317 (2011).
[47] K. Rudinger *et al.*, Phys. Rev. A **86**, 022334 (2012).
[48] A. M. Childs, D. Gosset, and Z. Webb, Science **339**, 791 (2013).
[49] C. J. Pethick and H. Smith, *Bose-Einstein Condensation in Dilute Gases* (Cambridge University Press, Cambridge, 2002).
[50] D. S. Abrams and S. Lloyd, Phys. Rev. Lett. **81**, 3992 (1998).
[51] O. Boada, A. Celi, J. I. Latorre, and M. Lewenstein, Phys. Rev. Lett. **108**, 133001 (2012).
[52] M. P. A. Fisher, P. B. Weichman, G. Grinstein, and D. S. Fisher, Phys. Rev. B **40**, 546 (1989).
[53] K. Sheshadri, H. R. Krishnamurthy, R. Pandit, and T. V. Ramakrishnan, Europhys. Lett. **257**, 22 (1993).
[54] J. F. Sherson *et al.*, Nature **467**, 68 (2010).
[55] P. Erdös, F. Harary, and W. T. Tutte, Mathematika **12**, 118 (1961).
[56] M. Fiedler, *Matrices and Graphs in Geometry* (Cambridge University Press, Cambridge, 2011).
[57] X. Lu, Y. Wang, M. Wu, and G. Jin, Opt. Commun. **72**, 157 (1989).
[58] P. Erdös and A. Rényi, Publ. Mathematicae **6**, 290 (1959).

[59] N. B. Lovett, M. Everitt, R. M. Heath, and Viv Kendon, arXiv:1110.4366.
[60] S. Raghavan, A. Smerzi, S. Fantoni, and S. R. Shenoy, Phys. Rev. A **59**, 620 (1999).
[61] J. R. Anglin, P. Drummond, and A. Smerzi, Phys. Rev. A **64**, 063605 (2001).
[62] S. H. Strogatz, *Nonlinear Dynamics and Chaos* (Westview Press, Boulder, CO, 1994).
[63] T. Anker *et al*., Phys. Rev. Lett. **94**, 020403 (2005).
[64] T. J. Alexander, E. A. Ostrovskaya, and Y. S. Kivshar, Phys. Rev. Lett. **96**, 040401 (2006).
[65] M. Fattori *et al*., Phys. Rev. Lett. **100**, 080405 (2008).
[66] J.-M. Hou, W.-X. Yang, and X.-J. Liu, Phys. Rev. A **79**, 043621 (2009).
[67] D. A. Meyer and T. G. Wong, New J. Phys. **15**, 063014 (2013).